Nonlinear inverse scattering and three-dimensional near-field optical imaging

George Y. Panasyuk
Department of Bioengineering, University of Pennsylvania, Philadelphia, Pennsylvania 19104

Vadim A. Markel
Department of Radiology, University of Pennsylvania, Philadelphia, Pennsylvania 19104

P. Scott Carney
Beckman Institute and Department of Electrical & Computer Engineering, University of Illinois, Urbana, Illinois 61801

John C. Schotland[a)]
Department of Bioengineering, University of Pennsylvania, Philadelphia, Pennsylvania 19104

(Received 18 September 2006; accepted 16 October 2006; published online 29 November 2006)

The nonlinear inverse scattering problem for electromagnetic fields with evanescent components is considered. A solution to this problem is obtained in the form of a functional series expansion. The first term in the expansion corresponds to the pseudoinverse solution to the linearized inverse problem. The higher order terms represent nonlinear corrections to this result. Applications to the problem of three-dimensional optical imaging with subwavelength resolution are described and illustrated with numerical simulations. © *2006 American Institute of Physics*.
[DOI: 10.1063/1.2396921]

Optical imaging at the nanoscale presents a formidable challenge with correspondingly great scientific rewards.[1] Of particular current interest is the possibility of three-dimensional nanoscale imaging.[2–4] Potential applications range across multiple fields within both the physical and biological sciences. In micro- and nanofabrication, for example, manufacturing processes are transitioning from planar to stacked platforms. In cell biology, the study of subcellular nanostructures is recognized as increasingly important. In these and numerous other examples, near-field microscopy realizes nanometer scale resolution but with a significant limitation, namely, only surface features of the sample are visualized.[3] Imaging of subsurface structures may be performed by a *destructive* method in which the sample is ablated and imaged layer by layer by scanning probe microscopy.[5]

Near-field tomography (NFT) is a recently proposed computed imaging modality for three-dimensional optical imaging with subwavelength resolution.[2,6–8] NFT is *nondestructive* and achieves nanoscale resolution by combining the experimental methods of near-field optics with the mathematical tools of inverse scattering theory. The diffraction limit to resolution is overcome by exploiting the ability of evanescent waves to carry information on subwavelength scales. In NFT the sample is illuminated sequentially by a series of incident waves while the scattered field is measured in the near zone. Using the data gathered from such an experiment, it is possible to reconstruct the three-dimensional sample structure as encoded by the spatial dependence of the susceptibility. This inverse scattering problem (ISP) has been studied within the accuracy of the single-scattering or first Born approximation.[6] The question of existence and uniqueness of solutions has been addressed, and computationally efficient inversion formulas are known.[2] The purpose of this letter is to extend these results to account for the effects of multiple scattering. This situation, in which the ISP is *nonlinear*, is of interest when variations in the susceptibility are not small or when the sample is sufficiently large—conditions which characterize a large class of physical systems.

We begin by considering the scattering of a monochromatic electromagnetic field from a nonmagnetic medium characterized by a position-dependent dielectric susceptibility $\eta(\mathbf{r})$. The electric field $\mathbf{E}$ is taken to consist of an incident part $\mathbf{E}^i$ and a scattered part $\mathbf{E}^s$ according to $\mathbf{E}=\mathbf{E}^i+\mathbf{E}^s$. The scattered field obeys the integral equation

$$E^s_\alpha(\mathbf{r}) = k_0^2 \int d^3r' G_{\alpha\beta}(\mathbf{r},\mathbf{r}') E_\beta(\mathbf{r}')\,\eta(\mathbf{r}'), \tag{1}$$

where $k_0=2\pi/\lambda$ is the free-space wave number, G denotes Green's tensor, and summation over repeated indices is implied. Evaluation of the integral in Eq. (1) is nontrivial since the scattered field appears on both the left- and right-hand sides of the equation. An explicit formula for $\mathbf{E}^s$, involving only the incident field, can be written in the form of the perturbation expansion,

$$\begin{aligned} E^s_\alpha(\mathbf{r}) = {} & k_0^2 \int d^3r' G_{\alpha\beta}(\mathbf{r},\mathbf{r}')\,\eta(\mathbf{r}') E^i_\beta(\mathbf{r}') \\ & + k_0^4 \int d^3r' d^3r'' G_{\alpha\beta}(\mathbf{r},\mathbf{r}')\,\eta(\mathbf{r}') G_{\beta\gamma}(\mathbf{r}',\mathbf{r}'')\,\eta(\mathbf{r}'') \\ & \times E^i_\gamma(\mathbf{r}'') + \cdots . \end{aligned} \tag{2}$$

The first term corresponds to single scattering of the incident field, the second term corresponds to double scattering, and so on. If the scattered field is much smaller than the incident field, then only the first term in Eq. (2) need be retained. This result, which is known as the first Born approximation, linearizes the integral equation (1) with respect to η. Note that

a)Electronic mail: schotland@seas.upenn.edu

multiple scattering leads to a nonlinear relationship between $\mathbf{E}$ and η.

The Green's tensor may be expanded into plane-wave modes of the form $G_{\alpha\beta}(\mathbf{r},\mathbf{r}')=1/(2\pi)^2\int d^2q\,\exp[i\mathbf{q}\cdot(\boldsymbol{\rho}-\boldsymbol{\rho}')]g_{\alpha\beta}(z,z';\mathbf{q})$, where we have used the notation $\mathbf{r}=(\boldsymbol{\rho},z)$ and the form of $g_{\alpha\beta}(z,z';\mathbf{q})$ is given in Ref. 2. Note that this decomposition facilitates the treatment of systems which are translationally invariant in the transverse direction and that the plane-wave modes are labeled by the transverse wave vector $\mathbf{q}$. The modes for which $|\mathbf{q}|\leqslant k_0$ correspond to propagating waves while the modes with $|\mathbf{q}|>k_0$ correspond to evanescent waves. The contribution of the evanescent modes is exponentially small in the far zone of the scatterer which leads to loss of high spatial-frequency information upon propagation.

We will assume that the sample occupies the region $0\leqslant z\leqslant L$ and that the scattered field is measured on the plane $z=z_d$ with $z_d>L$. The sample is illuminated by a plane wave of the form $\mathbf{E}^i=\mathbf{E}^{(0)}\exp(i\mathbf{q}_1\cdot\boldsymbol{\rho}+ik_z(\mathbf{q}_1)z)$ with polarization $\mathbf{E}^{(0)}$, transverse wave vector $\mathbf{q}_1$, and $k_z(\mathbf{q})=\sqrt{k_0^2-q^2}$. The scattered light is collected in the near zone of the sample by a small aperture in a probe tip which is scanned over a square lattice with lattice spacing h.

It will prove useful to define a data function by the lattice Fourier transform of the sampled scattered field, namely, $\Phi_\alpha(\mathbf{q}_1,\mathbf{q}_2)=\Sigma_{\boldsymbol{\rho}}e^{-i\mathbf{q}_2\cdot\boldsymbol{\rho}}E^s_\alpha(\boldsymbol{\rho},z_d;\mathbf{q}_1)$, where the sum is carried out over all lattice vectors, $\mathbf{q}_2$ belongs to the first Brillouin zone of the lattice, and the dependence on the incident transverse wave vector $\mathbf{q}_1$ has been made explicit. Making use of Eq. (2), we find that Φ can be represented in a convenient diagrammatic form:

$\boldsymbol{\Phi}=$ 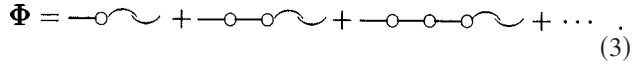 (3)

Diagrams through the third order of multiple scattering are shown and are to be understood as follows. A solid line corresponds to a factor of $k_0^2 g_{\alpha\beta}$, a wavy line to a factor of $(1/h^2)\exp(\pm ik_z(\mathbf{q})z)E^{(0)}_\alpha\equiv e_\alpha(\mathbf{q},z)$, and a circle to a factor of $\tilde{\eta}(\mathbf{q},z)=\int d^2\rho\,\exp(i\mathbf{q}\cdot\boldsymbol{\rho})\eta(\boldsymbol{\rho},z)$. In addition, a z integration is performed over each vertex and a $\mathbf{q}$ integration is carried out for every internal solid line. Applying these diagrammatic rules it can be seen that the first and second diagrams in Eq. (3) correspond to the integrals

$$k_0^2\int_0^L dz\sum_{\mathbf{Q}} g_{\alpha\beta}(z_d,z;\dot{\mathbf{q}}_1-\mathbf{q}_2)\tilde{\eta}(\mathbf{q}_2-\mathbf{Q},z)e_\beta(\mathbf{q}_1,z) \tag{4}$$

and

$$k_0^4\int_0^L\int_0^L dz_1dz_2\int\frac{d^2q}{(2\pi)^2}\sum_{\mathbf{Q}} g_{\alpha\beta}(z_d,z_1;\mathbf{q}_1-\mathbf{q}_2)\tilde{\eta}(\mathbf{q}-\mathbf{q}_1+\mathbf{q}_2-\mathbf{Q},z_1)g_{\beta\gamma}(z_1,z_2;\mathbf{q})\tilde{\eta}(\mathbf{q}_1-\mathbf{q},z_2)e_\gamma(\mathbf{q}_1,z_2), \tag{5}$$

where we have performed a shift in the argument of Φ so that $\mathbf{q}_2\rightarrow\mathbf{q}_1-\mathbf{q}_2$ and $\mathbf{Q}$ is a reciprocal lattice vector.

The inverse problem in NFT is to reconstruct $\tilde{\eta}$ from Φ. We begin by considering the linearized ISP. This corresponds to solving the integral equation $K_\alpha\tilde{\eta}=\Phi_\alpha$. Here the linear operator K_α is obtained by retaining only the first diagram in Eq. (2) and the action of K_α on $\tilde{\eta}$ is defined by the integral (4). The linearized inverse problem has the solution $\tilde{\eta}=K^+_\alpha\Phi_\alpha$, where K^+_α denotes the pseudoinverse of K_α which has been obtained elsewhere.[2,6] To derive the solution to the nonlinear ISP, we act on Eq. (2) with K^+ and thereby obtain

$\tilde{\eta}=\tilde{\eta}^{(1)}-K^+\Big($ 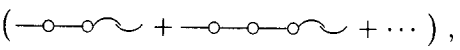 $\Big)$, (6)

where $\tilde{\eta}^{(1)}=K^+_\alpha\Phi_\alpha$. Next, we recognize that since Eq. (6) determines $\tilde{\eta}$ self-consistently, we can iterate this result and obtain a diagrammatic series for $\tilde{\eta}$ of the form

$\tilde{\eta}=$ 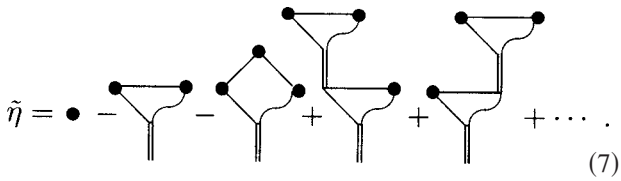 (7)

Here we have introduced the notation that $\tilde{\eta}^{(1)}=\bullet$, a double solid line represents K^+, and the effect of the overall application of K^+ is to join the ends of the diagrams. Applying the diagrammatic rules, it can be seen that the second diagram in Eq. (7) is given by the integral

$$k_0^4\int d^2q_1K^+_\alpha(z;\mathbf{q}_1,\mathbf{q}_2)\int_0^L\int_0^L dz_1dz_2\int\frac{d^2q}{(2\pi)^2}\sum_{\mathbf{Q}} g_{\alpha\beta}(z_d,z_1;\mathbf{q}_1-\mathbf{q}_2)\tilde{\eta}^{(1)}(\mathbf{q}-\mathbf{q}_1+\mathbf{q}_2-\mathbf{Q},z_1)g_{\beta\gamma}(z_1,z_2;\mathbf{q})\tilde{\eta}^{(1)}(\mathbf{q}_1-\mathbf{q},z_2)e_\gamma(\mathbf{q}_1,z_2). \tag{8}$$

We note that there are three diagrams of third order, seven of fourth order, and that the number of diagrams asymptotically doubles at each order.

Equation (7) provides a formally exact solution to the inverse problem of NFT. It may be viewed as a nonlinear inversion formula whose first term coincides with the pseudoinverse solution to the linearized ISP. The higher-order terms represent nonlinear corrections, which, in principle, can be computed to arbitrarily high order. We note that Eq. (7) implies that it is necessary only to solve the linear ISP in order to formally solve the nonlinear ISP.

Series solutions to the inverse problems of quantum mechanical backscattering, acoustic scattering, and optical tomography with diffuse light have been previously reported.[9–11] Though the algebraic structure of series solutions to different ISPs is similar, their analytic structure and convergence properties are quite different. This is a reflection of the underlying physical difference between the short-range propagation of evanescent waves in NFT and the long-range propagation of waves in quantum mechanics or acoustics. A detailed analysis of the convergence of the inverse series is beyond the scope of this letter. Finally, we stress that

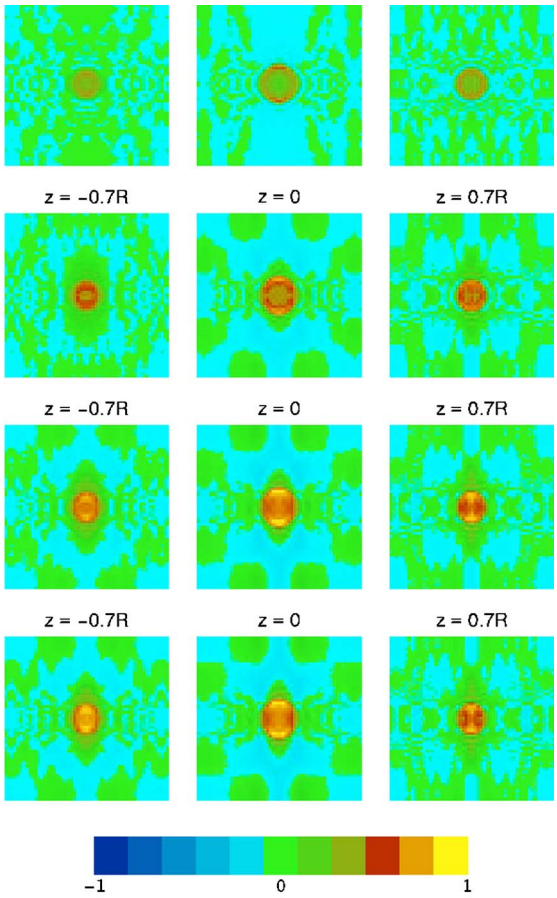

FIG. 1. (Color online) Tomographic images of a spherical scatterer. The field of view in each image is $18\lambda \times 18\lambda$.

the inverse series is a direct nonlinear inversion method, in contrast to iterative Newton-type methods,[12] which require the forward scattering problem to be solved for each iteration.

We now illustrate the use of the inverse series (7) with a numerical example. The scatterer consists of a sphere of radius $R=2\lambda$ with index of refraction $n=1.1$ related to the susceptibility by $\eta_0=(n^2-1)/4\pi$. The data function is computed from the Mie solution.[13] The incident field was polarized in the $\hat{\mathbf{x}}$ direction, and 31 incident plane waves were employed with transverse wave vectors pointing in the $\hat{\mathbf{y}}$ direction and ranging uniformly from $-0.9k_0\hat{\mathbf{y}}$ to $0.9k_0\hat{\mathbf{y}}$. The plane of detection was located at a distance $z_d=\lambda/3$ from the top of the sphere. The field was computed on a 600×600 grid with a lattice spacing $h=\lambda/6$. Figure 1 presents the reconstructions obtained. The central column shows the results of reconstructions in the equatorial plane of the sphere. The left and right columns are the results of reconstructions in the planes $0.7R$ above and below the equatorial plane. The first row illustrates the results of linear reconstructions while the second, third, and fourth rows show the second, third, and fourth order nonlinear reconstructions, respectively. Figure 2 shows the one-dimensional profiles of the reconstructed susceptibility along the line $y=0$ in the equatorial plane. All curves are normalized by the susceptibility η_0 of the sphere. It can be seen that the effect of the nonlinear corrections is to systematically improve the reconstructions order by order.

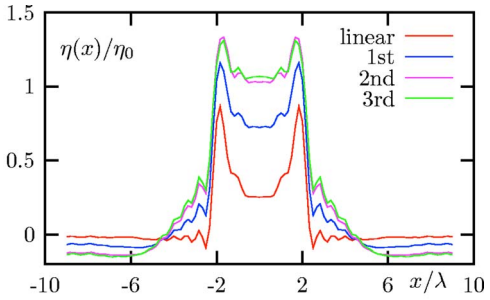

FIG. 2. (Color online) One-dimensional profiles of the reconstructed susceptibility.

In conclusion, we have described and illustrated in numerical simulations a nonlinear inverse scattering method for tomographic near-field optical imaging. We emphasize that our results provide a direct rather than a iterative numerical solution to the inverse problem. Applications to three-dimensional optical imaging of nanostructures are anticipated.

This work was supported by the NSF Grant No. DMR 0425780 to one of the authors (J.C.S.) and by the Air Force MURI Grant No. F49620-03-1-0379 to another author (P.S.C.).

[1] L. Novotny and B. Hecht, *Principles of Nano-Optics* (Cambridge University Press, New York, 2006).
[2] P. S. Carney and J. C. Schotland, MSRI Publications in Mathematics **47**, 133 (2003).
[3] T. Taubner, F. Keilmann, and R. Hillenbrand, Opt. Express **13**, 8893 (2005).
[4] N. Anderson, P. Anger, A. Hartschuh, and L. Novotny, Nano Lett. **6**, 744 (2006).
[5] R. Magerle, Phys. Rev. Lett. **85**, 2749 (2000).
[6] P. S. Carney and J. C. Schotland, Appl. Phys. Lett. **77**, 2798 (2000).
[7] P. S. Carney and J. C. Schotland, J. Opt. A, Pure Appl. Opt. **4**, S140 (2002).
[8] P. S. Carney, R. Frazin, S. Bozhevolnyi, V. Volkov, A. Boltasseva, and J. C. Schotland, Phys. Rev. Lett. **92**, 163903 (2004).
[9] R. T. Prosser, J. Math. Phys. **10**, 1819 (1969).
[10] A. B. Weglein, F. V. Arajo, P. M. Carvalho, R. H. Stolt, K. H. Matson, R. T. Coates, D. Corrigan, D. J. Foster, S. A. Shaw, and H. Zhang, Inverse Probl. **19**, R27 (2003).
[11] V. A. Markel, J. A. O'Sullivan, and J. C. Schotland, J. Opt. Soc. Am. A **20**, 903 (2003).
[12] W. C. Chew and Y. M. Wang, IEEE Trans. Med. Imaging **9**, 2318 (1990).
[13] C. F. Bohren and D. R. Huffman, *Absorption and Scattering of Light by Small Particles* (Wiley, New York, 1983).